

Causal Discovery with Multi-Domain LiNGAM for Latent Factors

Yan Zeng,^{1,2} Shohei Shimizu,^{2,3} Ruichu Cai,¹ Feng Xie,⁴
Michio Yamamoto,^{2,5} Zhifeng Hao^{1,6}

¹ Guandong University of Technology, China

² RIKEN Center for Advanced Intelligence Project (AIP), Japan

³ Shiga University, Japan ⁴ Peking University, China

⁵ Okayama University, Japan ⁶ Foshan University, China

Abstract

Discovering causal structures among latent factors from observed data is a particularly challenging problem, in which many empirical researchers are interested. Despite its success in certain degrees, existing methods focus on the single-domain observed data only, while in many scenarios data may be originated from distinct domains, e.g. in neuroinformatics. In this paper, we propose Multi-Domain Linear Non-Gaussian Acylic Models for Latent Factors (abbreviated as MD-LiNA model) to identify the underlying causal structure between latent factors (of interest), tackling not only single-domain observed data but multiple-domain ones, and provide its identification results. In particular, we first locate the latent factors and estimate the factor loadings matrix for each domain separately. Then to estimate the structure among latent factors (of interest), we derive a score function based on the characterization of independence relations between external influences and the dependence relations between multiple-domain latent factors and latent factors of interest, enforcing acyclicity, sparsity, and elastic net constraints. The resulting optimization thus produces asymptotically correct results. It also exhibits satisfactory capability in regimes of small sample sizes or highly-correlated variables and simultaneously estimates the causal directions and effects between latent factors. Experimental results on both synthetic and real-world data demonstrate the efficacy of our approach.

1 Introduction

Learning causal relationships from observed data, termed as causal discovery, has been developed over the past decades (Pearl 2000; Spirtes and Zhang 2016). In many scenarios, including sociology, psychology, and educational research, scientists are often interested in inferring causal relations between latent variables (or factors) that cannot be directly measured, e.g. anxiety, depression, or coping, etc (Silva et al. 2006; Bartholomew et al. 2008).

Some approaches have been developed to identify the causal structure between latent factors, which can be categorized into covariance-based and non-Gaussianity-based ones. Covariance-based methods employ firmly the covariance structure of data alone, e.g. BuildPureClusters algorithm (Silva et al. 2006), or FindOneFactorClusters algorithm (Kummerfeld and Ramsey 2016), to ascertain how many latent factors as well as the structure of latent factors. However, these algorithms can only output struc-

tures up to the Markov equivalence class for latent factors. Non-Gaussianity-based methods address this indistinguishable identification problem by taking the best of the non-Gaussianity of data. Specifically, Shimizu, Hoyer, and Hyvärinen (2009) leveraged non-Gaussianity and firstly achieved identifying a unique causal structure between latent factors based on the Linear, Non-Gaussian, Acyclic Models (LiNGAM) (Shimizu et al. 2006). They transformed the problem into the noisy ICA (Hyvarinen 1999). Recently, to avoid the local optima of the noisy ICA, Cai et al. (2019) designed the so-called Triad constraints, and proposed a two-phase method to learn the structure among latent factors.

The above-mentioned methods all focus on the data which are originated from the same domain, i.e. single-domain data. However, in many real-world applications, data are often collected under distinct conditions. They may be originated from different domains, resulting in distinct distributions and/or various causal effects. For instance, in neuroinformatics, functional Magnetic Resonance Imaging (fMRI) signals are frequently extracted from multiple subjects or over time (Smith et al. 2011). In biology, a particular disease is measured by distinct medical equipment (Dhir and Lee 2020); gene expression levels are measured under various experimental conditions (Shimamura et al. 2010), etc. Existing methods to handle multiple-domain data in causal discovery are flourishing, e.g. Danks, Glymour, and Tillman (2009); Tillman and Spirtes (2011); Shimizu (2012); Tillman and Eberhardt (2014); Ghassami et al. (2017, 2018); Dhir and Lee (2020); Huang et al. (2020). Though there are some methods to handle multiple-domain data that allow the existence of latent variables or confounders (Tillman and Spirtes 2011; Dhir and Lee 2020; Huang et al. 2020), no such method is yet proposed in the literature when learning the causal structure among latent factors, to our best knowledge. Thus, it is desirable to perform causal discovery from multiple-domain data to identify the structure among latent factors.

When considering multiple-domain instead of single-domain data, an important question naturally raises, i.e. how to guarantee that factors in different domains represent the same factors of interest. A solution may be to naively concatenate the multiple-domain observed data, such that the multi-domain model is regarded as a single-domain latent

factor model. However, it may cause serious bias in estimating the causal structure among latent factors of interest (Shimizu 2012). In this paper, we propose Multi-Domain Linear Non-Gaussian Acyclic Models for Latent Factors (namely MD-LiNA model) to represent the causal mechanism of multiple-domain data, which tackles not only single-domain data but multiple-domain ones. In addition, we propose an integrated two-phase approach to uniquely identify the underlying causal structure among latent factors (of interest). In particular, in the first phase, we locate the latent factors and estimate the factor loadings matrix (relating the observed variables to its latent factors) for each domain separately, which leverage the ideas from Triad constraints and factor analysis (Cai et al. 2019; Reilly and O’Brien 1996). In the second phase, we introduce a score function to characterize the independence relations between external variables, and interestingly, we unify this function to characterize the dependence relations between latent factors from different domains and latent factors of interest. Then such unified function is enforced with acyclicity, sparsity, and elastic net constraints, with which our task is formulated as a purely continuous optimization problem, which produces asymptotically correct results. Especially, our method also exhibits satisfactory capability in regimes of small sample sizes or highly-correlated variables and enables us to simultaneously estimate the causal directions and causal effects between latent factors.

Our contributions are mainly three-folded:

- We propose an MD-LiNA model, handling not only single-domain data, but multiple-domain ones, and show its identifiability results.
- We propose an integrated two-phase approach to *uniquely* estimate the underlying causal structure among latent factors, which simultaneously identifies not only causal directions but corresponding causal effects. It is capable of handling cases when the sample size is small or the latent factors are highly correlated.
- We provide its consistency, which is validated by simulation experiments and real-world applications.

2 Problem Formalization

Suppose we have data from M domains. Let $\mathbf{x}^{(m)}$, $\mathbf{f}^{(m)}$ ($m = 1, 2, \dots, M$) be the random vectors that collect observed variables and latent factors in domain m , respectively. The total number of observed variables for all domains is $p = \sum_{m=1}^M p_m$ while that of latent factors is $q = \sum_{m=1}^M q_m$. We assume the following data generation process,

$$\begin{aligned} \mathbf{f}^{(m)} &= \mathbf{B}^{(m)} \mathbf{f}^{(m)} + \boldsymbol{\varepsilon}^{(m)}, \\ \mathbf{x}^{(m)} &= \mathbf{G}^{(m)} \mathbf{f}^{(m)} + \mathbf{e}^{(m)}, \end{aligned} \quad (1)$$

where $\boldsymbol{\varepsilon}^{(m)}$, and $\mathbf{e}^{(m)}$ are random vectors that collect external influences, and errors, respectively, and all of them are independent with each other. $\mathbf{B}^{(m)}$ is a matrix that collects causal effects $b_{ij}^{(m)}$ between $f_i^{(m)}$ and $f_j^{(m)}$, while $\mathbf{G}^{(m)}$ collects factor loadings $g_{ij}^{(m)}$ between $f_j^{(m)}$ and $x_i^{(m)}$. Without

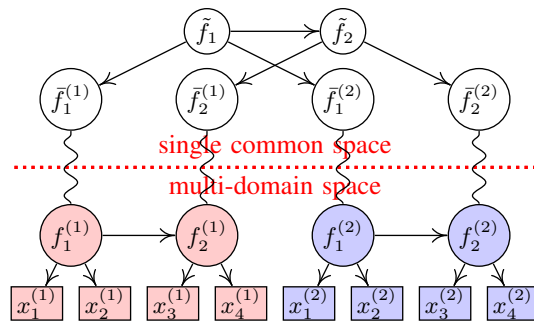


Figure 1: An MD-LiNA model. Variables in the same colors (light red and light blue) are in the same domain. Observed variables $\mathbf{x}^{(m)}$ in domain m entail its own latent factors $\mathbf{f}^{(m)}$. Augmented latent factors $\tilde{\mathbf{f}}$ are obtained using the coding representation method, which are signified by the curved wavy lines. $\tilde{\mathbf{f}}$ are latent factors of interest which generate $\tilde{\mathbf{f}}$ of different domains.

loss of generality, $f_i^{(m)}$ is assumed to have zero means and unit variances. Note that in each domain m , data are generated with the same causal effects $b_{ij}^{(m)}$, same loadings $g_{ij}^{(m)}$ and $\varepsilon_i^{(m)}$ and $e_i^{(m)}$ are sampled independently from the identical distributions.

Thereafter, we encounter two problems: how to integrate the multi-domain data efficiently; and how to guarantee factors $\mathbf{f}^{(m)}$ in different domains represent the same concepts (factors) of interest. Such problems prompt us to establish further for the model. To address the first problem, we leverage an idea of simple coding representation (Shimodaira 2016), i.e. an observation is represented as an augmented one with p dimensions, where only p_m dimensions come from the original domain while the other $(p - p_m)$ dimensions are padded with zeros. Any augmented data are expressed with a bar, e.g. $\bar{\mathbf{x}}$ and $\bar{\mathbf{f}}$. With such representations, we obtain,

$$\begin{aligned} \bar{\mathbf{f}} &= \bar{\mathbf{B}} \bar{\mathbf{f}} + \bar{\boldsymbol{\varepsilon}}, \\ \bar{\mathbf{x}} &= \bar{\mathbf{G}} \bar{\mathbf{f}} + \bar{\mathbf{e}}, \end{aligned} \quad (2)$$

where $\bar{\mathbf{G}} = \text{Diag}(\mathbf{G}^{(1)}, \dots, \mathbf{G}^{(M)}) \in \mathbb{R}^{p \times q}$, $\bar{\mathbf{B}} = \text{Diag}(\mathbf{B}^{(1)}, \dots, \mathbf{B}^{(M)})$, and $\bar{\boldsymbol{\varepsilon}}$ and $\bar{\mathbf{e}}$ are independent. A detailed explanation for this is presented in Supplementary Materials A. To address the second problem, we introduce factors of interest $\tilde{\mathbf{f}}$, which are embedded as different concepts with causal relations and generate $\tilde{\mathbf{f}}$. As depicted in Figure 1, suppose $\tilde{\mathbf{f}}$ are linearly generated by $\tilde{\mathbf{f}}$, i.e.

$$\tilde{\mathbf{f}} = \mathbf{H} \tilde{\mathbf{f}}, \quad (3)$$

where $\mathbf{H} \in \mathbb{R}^{q \times \tilde{q}}$ ($\tilde{q} \leq q$) is a transformation matrix, and \tilde{q} is the number of $\tilde{\mathbf{f}}$. The whole model is defined as follows.

Definition 1 (Multi-Domain LiNGAM for Latent Factors (MD-LiNA)). An MD-LiNA model satisfies the following assumptions:

- $\mathbf{f}^{(m)}$ are generated linearly from a Directed Acyclic Graph (DAG) with non-Gaussian distributed external variables $\boldsymbol{\varepsilon}^{(m)}$, as in Eq.(1);

- A2. $\mathbf{x}^{(m)}$ are generated linearly from $\mathbf{f}^{(m)}$ plus normally distributed errors $\mathbf{e}^{(m)}$, as in Eq.(1);
- A3. Each f_i has at least 2 pure measurement variables¹;
- A4. Each $\tilde{f}_i^{(m)}$ is linearly generated by only one latent in $\tilde{\mathbf{f}}$ and each \tilde{f}_i generates at least one latent in $\tilde{\mathbf{f}}$, as in Eq.(3).

Note that assumption A4 implies that each row of \mathbf{H} has only one non-zero element and each column has at least one non-zero element, which is explicable and mild. The key differences between MD-LiNA and the mostly common latent factor models are that $\mathbf{f}^{(m)}$ here may be causally related rather than being independent, allowing us to identify the causal structure among them; further, we introduce $\tilde{\mathbf{f}}$ and assumption A4, enabling us to handle multi-domain data.

Given single-domain data ($M = 1$), our goal is to estimate $\mathbf{G}^{(1)}$ and $\mathbf{B}^{(1)}$, where assumption A4 can be neglected and our model is simply called LiNGAM for LATent Factors (LiNA model); while given multi-domain data ($M > 1$), we aim to estimate $\mathbf{G}^{(m)}$ and $\tilde{\mathbf{B}}$ between factors of interest $\tilde{\mathbf{f}}$. Focusing on $\tilde{\mathbf{B}}$ offers a deeper interpretation of dependencies between observed variables across domains.

For a clear explanation, we use the **measurement model** to relate $\mathbf{x}^{(m)}$ to $\mathbf{f}^{(m)}$ while the **structure model** to record the causal relations among $\tilde{\mathbf{f}}$ or $\mathbf{f}^{(m)}$, following the definitions in (Spirtes, Glymour, and Scheines 2000; Silva et al. 2006).

3 Model Identification

In this section, we state our identifiability results. Note that the identifiability of single-domain LiNA models has been provided by Shimizu, Hoyer, and Hyvärinen (2009), but with the assumption that each latent factor has at least three pure measurement variables. Below we show that this identifiability can be strengthened to two pure variables by taking the best of Triad constraints (Cai et al. 2019), even when errors \mathbf{e} are Gaussian distributed but ε non-Gaussian.

Lemma 1. *Assume that the input data \mathbf{X} strictly follow the LiNA model. Let f_1 and f_2 be directed connected latent factors without confounders and let $\{x_i\}$ and $\{x_j, x_k\}$ be their pure measurement variables. Then $\{x_i, x_j\}$ and $\{x_k\}$ violate the Triad constraint if and only if $f_1 \rightarrow f_2$ holds.*

Note that the Triad constraints assume all noises including \mathbf{e} are non-Gaussian distributed. However, we allow \mathbf{e} are normally distributed in Lemma 1. With Lemma 1, we can enhance the identifiability to two pure variables for LiNA model. Next, we show that the identifiability of MD-LiNA model is further applicable, demonstrated in Theorem 1.

Theorem 1. *Assume that the input multiple-domain data \mathbf{X} with $\mathbf{X}^{(m)}$, $m = 1, \dots, M$ of domain m , strictly follow the MD-LiNA model. Then the underlying factor loadings matrix $\mathbf{G}^{(m)}$ is identifiable up to permutation and scaling of columns and the causal effects matrix $\tilde{\mathbf{B}}$ between factors of interest is fully identifiable as the sample size $n_m \rightarrow \infty$.*

¹Pure measurement variables are those which have only one single latent factor parent (Silva et al. 2006).

We give a sketch of the proof below. For complete proofs of all theoretical results, please see Supplementary Materials B.

Proof Sketch. According to the Triad constraints and Lemma 1, we guarantee the identifiability of LiNA model. For the MD-LiNA model, we have Eqs.(1), (2) and (3) to be satisfied. Then for each domain m in Eq.(1), as the sample size $n_m \rightarrow \infty$, $\mathbf{G}^{(m)}$ is identifiable up to permutation and scaling of columns, since we estimate the measurement models for each domain separately (mentioned in Section 4).

Furthermore, combining Eqs.(2) and (3), we obtain $\tilde{\mathbf{f}} = \tilde{\mathbf{B}}\tilde{\mathbf{f}} + \tilde{\varepsilon}$, where $\tilde{\mathbf{B}} = (\mathbf{H}^T \mathbf{H})^{-1} \mathbf{H}^T \tilde{\mathbf{B}} \mathbf{H} \in \mathbb{R}^{\tilde{q} \times \tilde{q}}$ and $\tilde{\varepsilon} = (\mathbf{H}^T \mathbf{H})^{-1} \mathbf{H}^T \tilde{\varepsilon} \in \mathbb{R}^{\tilde{q}}$. Note that the inverse matrix of $\mathbf{H}^T \mathbf{H}$ always exists since \mathbf{H} is full column rank due to the assumption A4. To prove $\tilde{\mathbf{B}}$ is identifiable, we have to additionally ensure $\tilde{\mathbf{B}}$ can be permuted to a strictly lower triangular matrix and $\tilde{\varepsilon}$ are independent with each other. Fortunately, due to assumption A1, $\tilde{\mathbf{B}}$ satisfies the condition. Due to assumption A4, by virtue of the independence between $\tilde{\varepsilon}$, its non-Gaussianity and the Darmois-Skitovich theorem (Darmois 1953; Skitovitch 1953), $\tilde{\varepsilon}$ are also independent with each other. Thus, $\tilde{\mathbf{B}}$ is fully identifiable, which implies the theorem is proved. \square

4 Model Estimation

We exhibit a two-phase framework (measurement-model and structure-model phases) to estimate causal structures under latent factors in Algorithm 1, and provide its consistency.

MD-LiNA Algorithm

In estimation, instead of learning all the matrices of interest at the same time, we derive an integrated two-phase framework, which not only facilitates the whole estimation procedure but also improves the accuracy.

For estimating measurement models, we have several approaches. Firstly, we can employ the Confirmatory Factor Analysis (CFA) approach (Reilly and O'Brien 1996), after using Triad constraints to yield the structure between latent factors $\mathbf{f}^{(m)}$ and observed variables $\mathbf{x}^{(m)}$ (Cai et al. 2019). Secondly, more exploratory approaches are advocated, e.g. Exploratory Structural Equation Modeling (ESEM) approach (Asparouhov and Muthén 2009), which enables us to use fewer restrictions on estimating factor loadings. Please see Supplementary Materials C for details. In our paper, we take the first approach, as illustrated in lines 1 to 3 of Algorithm 1, but we can use the second one as well in our framework. Note that we estimate the measurement models for each domain separately.

Below we give all the details for estimating structure models. We first introduce the log-likelihood function of LiNA model, enforcing various types of constraints to strengthen its learning power for different cases. Then we unify it into MD-LiNA model so as to address the problem about how to guarantee that factors in different domains represent the same factors. For brevity, we omit the superscripts of all notations for LiNA models with $M = 1$.

The log-likelihood function of LiNA model is derived by characterizing the independence relations between ε ,

$$\begin{aligned} \mathcal{L}(\mathbf{B}, \hat{\mathbf{G}}) = & \sum_{t=1}^n \left[\frac{1}{2} \left\| \mathbf{X}(t) - \hat{\mathbf{G}} \tilde{\mathbf{G}}^T \mathbf{X}(t) \right\|_{\Sigma^{-1}}^2 \right. \\ & \left. + \sum_{i=1}^q \log \hat{p}_i(\mathbf{g}_i^T \mathbf{X}(t) - \mathbf{b}_i^T \tilde{\mathbf{G}}^T \mathbf{X}(t)) \right] + C, \end{aligned} \quad (4)$$

where $\|\mathbf{x}\|_{\Sigma^{-1}}^2 = \mathbf{x}^T \Sigma^{-1} \mathbf{x}$, $\mathbf{X}(t)$ is the t^{th} column (observation) of data \mathbf{X} . $\tilde{\mathbf{G}}^T = (\hat{\mathbf{G}}^T \hat{\mathbf{G}})^{-1} \hat{\mathbf{G}}^T$ relates to the estimated $\hat{\mathbf{G}}$ and \mathbf{g}_i is the i^{th} column of $\tilde{\mathbf{G}}$. The inverse matrix of $\hat{\mathbf{G}}^T \hat{\mathbf{G}}$ always exists due to assumption A3. \mathbf{b}_i denotes the i^{th} column of \mathbf{B} . n is the sample size. C is a constant and \hat{p}_i is their corresponding density function. Please see Supplementary Materials D.1 for detailed derivations.

We derive such log-likelihood function, other than directly applying least-squares loss functions or other types, which enjoys the following merits: i) A dominating benefit of our formulation is the binding of likelihood with ε . It enables us to company ε with the independence constraints, so that they can be directly dealt with as an optimization problem by manipulating ε 's estimation. However, other loss functions can not convey such information. ii) It belongs to a semi-parametric problem since the densities of ε are not specified. But, there are various available estimation methods for approximating $\log \hat{p}_i$ (Pham and Garat 1997). It has been realized that even when fixing \hat{p}_i to be a single function, one can still receive a consistent and satisfactory estimator (Hyvärinen et al. 2010; Cardoso and Laheld 1996). In the experiments, we simply use a symmetric super-Gaussian distribution, i.e., the Laplace distribution, to model \hat{p}_i (Hyvärinen and Smith 2013).

Further, to guarantee the causal structure among latent factors is always acyclic and sparse, and to tackle multicollinearity problem, we render \mathbf{B} to satisfy an acyclicity constraint, adaptive ℓ_1 as well as ℓ_2 regularizations (Zheng et al. 2018; Hyvärinen et al. 2010; Zou and Hastie 2005),

$$\min_{\mathbf{B}} \mathcal{F}(\mathbf{B}, \hat{\mathbf{G}}), \quad \text{s.t.} \quad h(\mathbf{B}) = 0,$$

$$\text{where} \quad \mathcal{F}(\mathbf{B}, \hat{\mathbf{G}}) = -\mathcal{L}(\mathbf{B}, \hat{\mathbf{G}}) + \lambda_1 \|\mathbf{B}\|_{1*} + \lambda_2 \|\mathbf{B}\|^2, \quad (5)$$

$h(\mathbf{B}) = \text{tr}(e^{\mathbf{B} \circ \mathbf{B}}) - q$ is the acyclicity constraint, \circ is the Hadamard product, and $e^{\mathbf{B}}$ is the matrix exponential of \mathbf{B} . $\|\mathbf{B}\|_{1*} = \sum_{i=1}^q \sum_{j=1}^q |b_{ij}| / |\hat{b}_{ij}|$ represents the sparsity constraint where \hat{b}_{ij} in $\hat{\mathbf{B}}$ is estimated by maximizing $\mathcal{L}(\mathbf{B}, \hat{\mathbf{G}})$. $\|\mathbf{B}\|^2$ is the ℓ_2 regularization. λ_1 and λ_2 are regularization parameters. This optimization function facilitates us to simultaneously learn causal directions and effects between latent factors, without additional steps of permutation and rescaling, as required in Shimizu, Hoyer, and Hyvärinen (2009), which may lack statistical efficiency. The sparsity enables us to handle cases where the sample sizes are small.

Thus, with estimated $\hat{\mathbf{G}}$, we leverage the augmented Lagrangian method to optimize \mathbf{B} , transforming the con-

strained problem into an unconstrained one,

$$\min_{\mathbf{B}} \mathcal{S}(\mathbf{B}), \quad (6)$$

in which $\mathcal{S}(\mathbf{B}) = \mathcal{F}(\mathbf{B}, \hat{\mathbf{G}}) + \frac{\rho}{2} h(\mathbf{B})^2 + \alpha h(\mathbf{B})$ is the augmented Lagrangian. ρ and α represent a regularization parameter and Lagrange multiplier, respectively. Consequently, Eq.(6) is solved by adopting an efficient numerical algorithm, namely L-BFGS-B (Zhu et al. 1997). In case of avoiding numerical false discoveries from the estimation, it is a good strategy to rule out those edges whose estimated effects are under a small threshold ϵ (Zheng et al. 2018).

Now we show how Eq.(5) is unified to handle multiple-domain cases ($M > 1$) in a consistent way. In the first phase, all $\hat{\mathbf{f}}^{(m)}$ are projected as $\tilde{\mathbf{f}}$ into a single common space. Then, we introduce the dependence relations between $\tilde{\mathbf{f}}$ and $\tilde{\mathbf{f}}$ ($\tilde{\mathbf{f}} = \mathbf{H} \tilde{\mathbf{f}}$) to guarantee that factors from different domains represent the same concept or factor of interest. Thus, to learn the transformation matrix \mathbf{H} , we add reconstruction errors $\mathcal{E}(\mathbf{H})$ and an adaptive sparsity $\|\mathbf{H}\|_{1*}$ into Eq.(5), i.e.

$$\min_{\tilde{\mathbf{B}}, \mathbf{H}} \bar{\mathcal{F}}(\tilde{\mathbf{B}}, \mathbf{H}), \quad \text{s.t.} \quad h(\tilde{\mathbf{B}}) = 0,$$

$$\text{where} \quad \bar{\mathcal{F}}(\tilde{\mathbf{B}}, \mathbf{H}) = \mathcal{F}(\tilde{\mathbf{B}}, \mathbf{H}) + \mathcal{E}(\mathbf{H}) + \lambda_3 \|\mathbf{H}\|_{1*}, \quad (7)$$

$\mathcal{E}(\mathbf{H}) = \|\tilde{\mathbf{f}} - \mathbf{H} \tilde{\mathbf{f}}\|^2 = \|\tilde{\mathbf{f}} - \mathbf{P}_{\mathbf{H}} \tilde{\mathbf{f}}\|^2$ is reconstruction error, $\mathbf{P}_{\mathbf{H}} = \mathbf{H}(\mathbf{H}^T \mathbf{H})^{-1} \mathbf{H}^T$ is the projection matrix onto the column space of \mathbf{H} , and λ_3 is a regularization parameter. $\mathcal{F}(\tilde{\mathbf{B}}, \mathbf{H})$ contains the log-likelihood of MD-LiNA model,

$$\begin{aligned} \mathcal{F}(\tilde{\mathbf{B}}, \mathbf{H}) = & -\mathcal{L}(\tilde{\mathbf{B}}, \mathbf{H}) + \lambda_1 \|\tilde{\mathbf{B}}\|_{1*} + \lambda_2 \|\tilde{\mathbf{B}}\|^2, \\ = & -\sum_{m=1}^M \sum_{t=1}^n \left[\frac{1}{2} \left\| \mathbf{X}^{(m)}(t) - \hat{\mathbf{G}}^{(m)} \tilde{\mathbf{G}}^{(m)T} \mathbf{X}^{(m)}(t) \right\|_{\Sigma^{-1}}^2 \right. \\ & \left. + \sum_{i=1}^{\tilde{q}} \log \hat{p}_i(\mathbf{h}_i^T \tilde{\mathbf{f}}(t) - \tilde{\mathbf{b}}_i^T \tilde{\mathbf{H}}^T \tilde{\mathbf{f}}(t)) \right] - C \\ & + \lambda_1 \|\tilde{\mathbf{B}}\|_{1*} + \lambda_2 \|\tilde{\mathbf{B}}\|^2, \end{aligned} \quad (8)$$

where $\tilde{\mathbf{G}}^{(m)T} = (\hat{\mathbf{G}}^{(m)T} \hat{\mathbf{G}}^{(m)})^{-1} \hat{\mathbf{G}}^{(m)T}$, $\tilde{\mathbf{H}}^T = (\mathbf{H}^T \mathbf{H})^{-1} \mathbf{H}^T$, the inverse matrices of $\mathbf{H}^T \mathbf{H}$ and $\hat{\mathbf{G}}^{(m)T} \hat{\mathbf{G}}^{(m)}$ always exist due to assumptions A3 and A4 and \mathbf{h}_i is the i^{th} column of $\tilde{\mathbf{H}}$. $\tilde{\mathbf{b}}_i$ denotes the i^{th} column of $\tilde{\mathbf{B}}$. See Supplementary Materials D.2 for detailed derivations.

We optimize iteratively \mathbf{H} and $\tilde{\mathbf{B}}$ using augmented Lagrangian method until convergence. Specifically, i) to optimize \mathbf{H} , we find its descent direction to derive the next iteration for a given $\tilde{\mathbf{B}}$. Since there is no constraints for \mathbf{H} , it is an unconstrained problem. ii) to optimize $\tilde{\mathbf{B}}$, we compute its descent direction for the next iteration given \mathbf{H} , and update the Lagrange multiplier α . $\tilde{\mathbf{B}}$ and α are iteratively updated until the acyclicity constraint $h(\tilde{\mathbf{B}}) = 0$ is satisfied. Finally, we repeat the steps i) and ii) until $\tilde{\mathbf{H}}$ and $\tilde{\mathbf{B}}$ are convergent. With $\tilde{\mathbf{H}}$, we can link the factors from multiple

Algorithm 1 MD-LiNA Algorithm

Input: Data $\mathbf{X}^{(1)}, \dots, \mathbf{X}^{(M)}$; M .
Output: Factor loadings $\hat{\mathbf{G}}^{(m)}$ ($\hat{\mathbf{G}}$); effects matrix $\hat{\mathbf{B}}$ ($\hat{\mathbf{B}}$).
Phase I: Measurement models
1: Find the number of latent factors q_m and pure clusters $\mathbf{P}c_m$ for each domain m using $\mathbf{X}^{(m)}$ by Triad constraints, and estimate $\hat{\mathbf{G}}^{(m)}$ by CFA;
2: Estimate $\hat{\mathbf{f}}^{(m)} \doteq (\hat{\mathbf{G}}^{(m)T} \hat{\mathbf{G}}^{(m)})^{-1} \hat{\mathbf{G}}^{(m)T} \mathbf{X}^{(m)}$;
3: Get augmented data $\tilde{\mathbf{f}} = \text{Diag}(\hat{\mathbf{f}}^{(1)}, \dots, \hat{\mathbf{f}}^{(M)})$;
Phase II: Structure models
4: **if** $M > 1$ **then**
5: Optimize Eq.(7) iteratively for $\hat{\mathbf{H}}$ and $\hat{\mathbf{B}}$ until convergence using augmented Lagrangian method;
6: Update $\hat{\mathbf{B}}$ with regard to $\hat{\mathbf{H}}$;
7: **else**
8: Optimize Eq.(5) to get $\hat{\mathbf{B}}$ with augmented Lagrangian method, with $\hat{\mathbf{G}} = \hat{\mathbf{G}}^{(1)}$;
9: **end if**
10: **return** $\hat{\mathbf{G}}^{(m)}$ and $\hat{\mathbf{B}}$ ($M > 1$); or $\hat{\mathbf{G}}$ and $\hat{\mathbf{B}}$ ($M = 1$).

domains with high weights together to symbolize the same concepts so that we can decide which factors from different domains are represented by which factors of interest. Specifically, for \tilde{f}_i , those factors $\tilde{\mathbf{f}}$ from different domains with the largest weights are considered to be represented by this \tilde{f}_i , where \tilde{f}_i can also be named according to its corresponding observed measurement variables. Then according to these represented factors $\tilde{\mathbf{f}}$ for each \tilde{f}_i , we obtain the causal ordering among $\tilde{\mathbf{f}}$, with which the $\hat{\mathbf{B}}$ can be updated.

Consistency Proofs

Here we prove that our methods could provide consistent estimators for MD-LiNA models, including LiNA models.

Theorem 2. *Assume that the input single-domain data \mathbf{X} strictly follow the LiNA model. With the factor analysis and the likelihood accompanied with the acyclicity constraint as a score function in Eq.(5), cast as a constrained optimization, our method guarantees to learn $\hat{\mathbf{G}}$ and $\hat{\mathbf{B}}$ which are consistent to the true \mathbf{G} and \mathbf{B} asymptotically, respectively.*

Theorem 3. *Assume that the input multiple-domain data \mathbf{X} with $\mathbf{X}^{(m)}$, $m = 1, \dots, M$ of domain m , strictly follow the MD-LiNA model. With the likelihood and construction error accompanied with the acyclicity constraint as a score function in Eq.(7), cast as a constrained optimization, our method guarantees to learn $\hat{\mathbf{G}}^{(m)}$, $\hat{\mathbf{H}}$ and $\hat{\mathbf{B}}$ which are consistent to the true $\mathbf{G}^{(m)}$, \mathbf{H} and \mathbf{B} asymptotically, respectively.*

Theorems 2 and 3 ensure that with proper score functions and constraints for MD-LiNA models, asymptotically the resulting estimators are consistent with those generated true ones. The proofs are shown in Supplementary Materials B.3 and B.4.

5 Experiments

We applied our methods to synthetic and real-world data to learn causal graphs between latent factors. Since existing methods focus on single-domain data only, experiments conducted here include multiple-domain data as well as single-domain ones for fair comparisons. Further, due to the unstable performance of Triad constraints to find pure clusters, we assume that the structure in measurement models is known a prior for all methods, including compared ones.

Synthetic Data

Taking a LiNA model as an example, we generated the data according to Eq.(1), i.e. firstly the structure models and secondly the measurement models. Unless specified, each generated structure has 5 latent factors and each factor measures two pure variables with sample size 1000. Please see Supplementary Materials E.1 for detailed descriptions and experimental settings. We performed experiments with **i) different sample sizes; ii) highly-correlated latent variables; iii) multi-domain data** and **iv) different numbers of latent factors**. For the robustness performances with **v) different noise ratios, vi) different regularization parameters** and **vii) different non-Gaussian distributions** of the noises of latent factors, please see Supplementary Materials E.2.

We compared our method with NICA based on the noisy ICA (Shimizu, Hoyer, and Hyvärinen 2009) and Triad (Cai et al. 2019). Since Triad outputs causal directions of latent factors with no causal effects, we used the recall, precision, and F1 score as measurements to evaluate the difference between the estimated skeleton and the true one. F1 score is a weighted average of recall and precision, with $\text{F1 score} = 2 \times \text{recall} \times \text{precision} / (\text{recall} + \text{precision})$. Besides, since NICA aimed to estimate both causal directions and causal effects between latent factors but not simultaneously, we exploited scatter plots between the estimated matrices and the true ones for another accuracy measurement.

Firstly, we generated the data **i) with different sample sizes** $n = 100, 200, 500, 1000, 2000$, to verify the capability in small-sample-size schemes. Figure 2(a)(b)(c) depicts the recall, precision and F1 scores of the learned causal graphs. Overall, we found that our LiNA always achieves the best performance, especially with smaller sample sizes. In detail, as sample sizes decrease, performances of other methods decrease whereas LiNA remains incredibly preponderant, showing its robustness. In regard to the Triad method, although its recall is comparable to ours with enough sample sizes, its precision is always the worst, even with increasing sample sizes. The reason may be that the sample sizes are not adequate for Triad to prune the causal directions, resulting in the output graph with many redundant edges.

Secondly, we generated **ii) highly-correlated variables** through simulating different ranges of weights of latent factors $[-i, -0.5] \cup [0.5, i]$, $i = 2, \dots, 6$, represented as i . Their corresponding average Variable Inflation Factors (VIF)² are 22%, 47%, 69%, 78% and 84%, respectively, which measure the multicollinearity of variables and higher VIFs mean

²Average Variable Inflation Factors (VIF) are defined as the average VIF for all 100 independent trials of each range of weights.

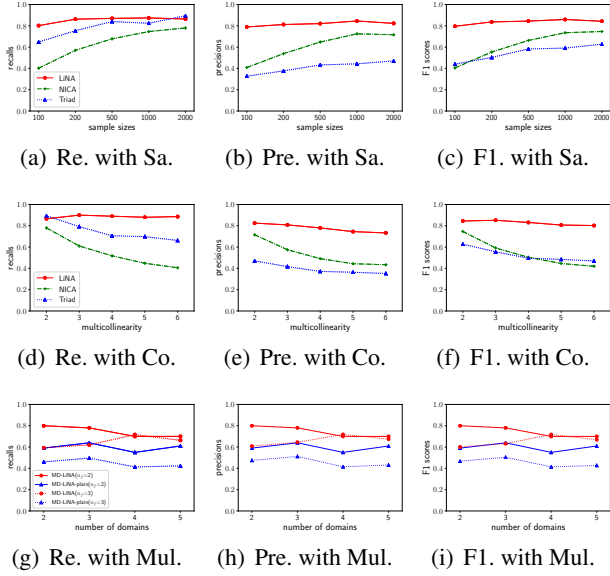


Figure 2: The recall (Re.), precision (Pre.) and F1 scores (F1.) of the recovered causal graphs between latent factors with different sample sizes (Sa.) i.e. $n=100, 200, 500, 1000, 2000$ in (a), (b) and (c), whose noises of latent factors follow Laplace distributions; with different levels of multicollinearities (Co.) in (d), (e) and (f). In particular, in the x-axis, levels of multicollinearities of $i = 2, \dots, 6$ are 22%, 47%, 69%, 78% and 84%, respectively, in the average VIF; and with different numbers of domains (Mul.) in (g), (h) and (i). Higher F1 score represents higher accuracy.

the heavier multicollinearity. In Figure 2(d)(e)(f), we found as VIF increases, the accuracy of all methods declines in different degrees, but our method is the most robust to the high multicollinearity and thus outperforms the other comparisons, which is due to the employment of the elastic net regularization and verifies its significant roles.

Thirdly, we generated **iii) multi-domain data** $M = 2, 3, 4, 5$, through varying noises ε 's distributions from sub-Gaussian or super-Gaussian ones. For each domain m , we generated the identical sample size 1000, the identical number of latent factors n_f , and the identical causal graphs of latent factors, as it is a straightforward way to obtain the true skeleton for evaluation. For further justification of efficacy, we also varied the numbers of latent factors $n_f = 2, 3$. Since NICA and Triad do not focus on multiple-domain data, we used our method which did not conduct line 6 of Algorithm 1 as the comparison, namely MD-LiNA-plain method. That is, after getting \hat{B} and \hat{H} , MD-LiNA-plain did not update \hat{B} according to \hat{H} . As shown in Figure 2(g)(h)(i), the x-axis stands for the number of domains. Overall, we found that F1 scores of both methods tend to decrease as the number of domains or the number of latent factors increases. Specifically, in all cases our MD-LiNA always gives a better performance compared with MD-LiNA-plain, in that MD-LiNA-plain did neglect the problem that factors from different domains are

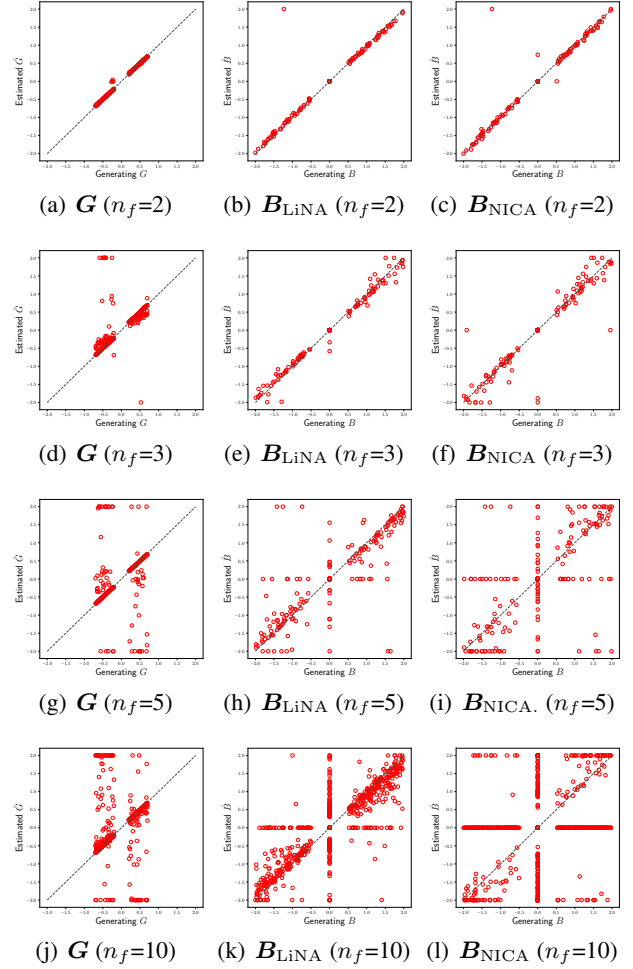


Figure 3: Scatter plots of estimated causal structures versus the true causal structures with different numbers of latent factors ($n_f=2,3,5,10$). It is worth noting that estimates outside the interval $[-2,2]$ are plotted at the edges of this interval for the sake of clearer demonstration. (a), (d), (g) and (j) are scatter plots of the estimated factor loading values \hat{g}_{ij} in \hat{G} versus the true ones. (b), (e), (h) and (k) are scatter plots of our method's estimated causal effects \hat{b}_{ij} in the adjacency matrix \hat{B} versus the true ones while (c), (f), (i) and (l) are of NICA method's estimated causal effects \hat{b}_{ij} . The x-axis is the generating G or B while the y-axis is the estimated \hat{G} or \hat{B} . Closer to the main diagonal means higher accuracy.

represented by which factors of interest, and it did not update the \hat{B} . Such experiments confirm the efficacy of our method and the necessity and significance of updating \hat{B} with \hat{H} .

Finally, to emphasize the capability of estimating causal effects, we conducted experiments with **iv) different numbers of latent factors** $n_f = 2, 3, 5, 10$, compared with NICA. Each latent factor has two pure measurement variables. Figure 3 demonstrates the scatter plots of estimated

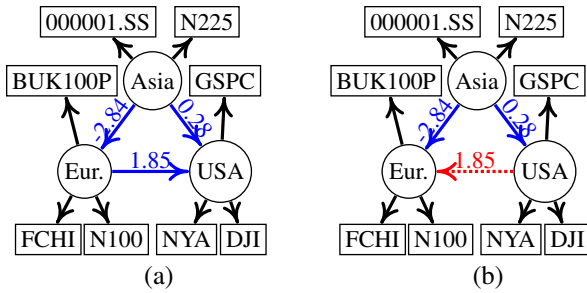


Figure 4: Estimated stock indices networks using the (a) MD-LiNA and (b) MD-LiNA-plain methods. Solid blue lines denote consistent edges with the ground truth while densely dotted red lines are not.

causal structures versus the true ones. The x-axis is the generating G or B while the y-axis is the estimated \hat{G} or \hat{B} . Closer to the main diagonal means higher accuracy. Note that we applied the identical method, CFA, to estimate \hat{G} as the NICA. Using the same estimated \hat{G} allows us to see how estimation errors from \hat{G} may propagate and influence the estimation of \hat{B} . Overall, we found that our LiNA gives better performances in all cases with different numbers of latent factors. The accuracy decreases along with the increasing number of latent factors and the fixed sample size. More specifically, when there are 2 latent factors $n_f=2$, NICA is comparable to ours. However, as $n_f=10$, accuracies of both methods decrease, but our LiNA decreases much more slowly than NICA. The reasons may be that 1) the increasing number of measurement variables with the fixed sample size results in reduced power of CFA to estimate \hat{G} , propagating errors to the final learning of \hat{B} ; 2) our method enforces a sparsity constraint, which enables us to deal with data with small sample sizes while NICA does not. And NICA does not estimate the causal directions and effects simultaneously, either, which may lack statistical efficiency and induce additional errors.

Real-World Applications

Yahoo stock indices dataset. We aimed to discover the causal structure in the daily stock returns between different regions of the world, i.e. Asia, Europe, and the USA, each of which consisted of 2 or 3 stock indices. They were Asia := {N225, 000001.SS} from Japan and China, Europe := {BUK100P, FCHI, N100} from United Kingdom, France, and other European countries, and USA := {DJI, GSPC, NYA} from the United States. To verify the efficacy of MD-LiNA schemes, we divided the data into two non-overlapping time segments such that their distributions varied across segments and are viewed as two different domains. We tested its multicollinearity and used 10-fold cross validation to select parameter values. More details can be seen in Supplementary Materials F.1.

Figure 4 shows the resulting graph employing the MD-LiNA method (Figure 4(a)) and MD-LiNA-plain method (Figure 4(b)). Due to the different time zones, it is expected

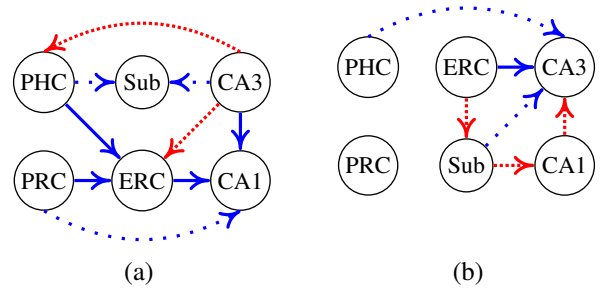


Figure 5: Causal structures learned from fMRI hippocampus data using (a) our LiNA and (b) NICA methods. Solid blue lines represent consistent edges with the anatomical connectivity while densely dotted red lines are spurious and not consistent. Loosely dotted blue lines represent redundant edges.

that the ground truth is Asia \rightarrow Europe \rightarrow USA (Janzing, Hoyer, and Schölkopf 2010; Chen et al. 2014). Thus, we found that the recovered causal structure of our method was in accordance with the ground truth while the plain one was not.

fMRI hippocampus dataset. We are interested in investigating causal relations between six brain regions of an individual: perirhinal cortex (PRC), parahippocampal cortex (PHC), entorhinal cortex (ERC), subiculum (Sub), CA1, and CA3/Dentate Gyrus (DG), each of which had both left and right sides and were treated as measurements (Poldrack et al. 2015). We used the anatomical connectivity between regions as a reference to evaluate the estimated structures. (Bird and Burgess 2008; Ghassami et al. 2018). For more experimental information please refer to Supplementary Materials F.2.

The resulting graphs are demonstrated in Figure 5. Edges consistent with the anatomical connectivity are highlighted with solid blue lines while those with loosely dotted blue lines represent redundant edges. Edges that are spurious and not consistent are highlighted with densely dotted red lines. From Figure 5, we see that though our method estimated one more redundant edge, we obtained more consistent as well as less spurious edges than the NICA method. Besides, we found that our results also coincide with some current findings. For example, the relation CA3 \rightarrow CA1 is declared connective in neuroscience (Song et al. 2015); PRC \rightarrow ERC and PHC \rightarrow ERC are usually related to episodic memories, which suggest distinct roles in memory formation and retrieval (Kuhn et al. 2018); and ERC \rightarrow CA1 is supposed to correlate with memory loss (Kerchner et al. 2012).

6 Conclusions

In this paper, we proposed Multi-Domain Linear Non-Gaussian Acyclic Models for Latent Factors (called MD-LiNA model), tackling not only single-domain data but multiple-domain ones, and provide its identification results. Additionally, we proposed an integrated two-phase approach to discover the causal directions as well as causal effects between latent factors simultaneously, in contrast with the existing methods that perform these estimations in succession.

It can also handle cases where the sample size is small or the latent factors are highly correlated. Our experimental results on simulated data and real-world applications validated the effectiveness and efficacy of the proposed algorithm.

References

- Asparouhov, T.; and Muthén, B. 2009. Exploratory structural equation modeling. *Structural Equation Modeling: A Multidisciplinary Journal* 16(3): 397–438.
- Bartholomew, D.; Steele, F.; Moustaki, I.; and Galbraith, J. 2008. *The Analysis and Interpretation of Multivariate Data for Social Scientists*. Routledge (2 edition).
- Bird, C. M.; and Burgess, N. 2008. The hippocampus and memory: insights from spatial processing. *Nature Reviews Neuroscience* 9(3): 182–194.
- Cai, R.; Xie, F.; Glymour, C.; Hao, Z.; and Zhang, K. 2019. Triad Constraints for Learning Causal Structure of Latent Variables. In *Advances in Neural Information Processing Systems (NeurIPS)*, 12863–12872.
- Cardoso, J.-F.; and Laheld, B. H. 1996. Equivariant adaptive source separation. *IEEE Transactions on Signal Processing* 44(12): 3017–3030.
- Chen, Z.; Zhang, K.; Chan, L.; and Schölkopf, B. 2014. Causal discovery via reproducing kernel hilbert space embeddings. *Neural Computation* 26(7): 1484–1517.
- Danks, D.; Glymour, C.; and Tillman, R. E. 2009. Integrating locally learned causal structures with overlapping variables. In *Advances in Neural Information Processing Systems (NIPS)*, 1665–1672.
- Darmois, G. 1953. Analyse générale des liaisons stochastiques. *Review of the International Statistical Institute* 21: 2–8.
- Dhir, A.; and Lee, C. M. 2020. Integrating Overlapping Datasets Using Bivariate Causal Discovery. In *Proceedings of the 34th AAAI Conference on Artificial Intelligence (AAAI)*, 3781–3790.
- Ghassami, A.; Kiyavash, N.; Huang, B.; and Zhang, K. 2018. Multi-domain causal structure learning in linear systems. In *Advances in Neural Information Processing Systems (NeurIPS)*, 6266–6276.
- Ghassami, A.; Salehkaleybar, S.; Kiyavash, N.; and Zhang, K. 2017. Learning causal structures using regression invariance. In *Advances in Neural Information Processing Systems (NIPS)*, 3011–3021.
- Huang, B.; Zhang, K.; Gong, M.; and Glymour, C. 2020. Causal Discovery from Multiple Data Sets with Non-Identical Variable Sets. In *Proceedings of the 34th AAAI Conference on Artificial Intelligence (AAAI)*, 10153–10161.
- Hyvärinen, A. 1999. Gaussian moments for noisy independent component analysis. *IEEE Signal Processing Letters* 6(6): 145–147.
- Hyvärinen, A.; and Smith, S. M. 2013. Pairwise likelihood ratios for estimation of non-Gaussian structural equation models. *Journal of Machine Learning Research* 14(1): 111–152.
- Hyvärinen, A.; Zhang, K.; Shimizu, S.; and Hoyer, P. O. 2010. Estimation of a structural vector autoregression model using non-gaussianity. *Journal of Machine Learning Research* 11(5): 1709–1731.
- Janzing, D.; Hoyer, P. O.; and Schölkopf, B. 2010. Telling cause from effect based on high-dimensional observations. In *Proceedings of the 27th International Conference on Machine Learning (ICML)*, 479–486. Omnipress.
- Kerchner, G. A.; Deutsch, G. K.; Zeineh, M.; Dougherty, R. F.; Saranathan, M.; and Rutt, B. K. 2012. Hippocampal CA1 apical neuropil atrophy and memory performance in Alzheimer’s disease. *Neuroimage* 63(1): 194–202.
- Kuhn, T.; Gullett, J. M.; Boutzoukas, A. E.; Bohsali, A.; Mareci, T. H.; FitzGerald, D. B.; Carney, P. R.; and Bauer, R. M. 2018. Temporal lobe epilepsy affects spatial organization of entorhinal cortex connectivity. *Epilepsy & Behavior* 88: 87–95.
- Kummerfeld, E.; and Ramsey, J. 2016. Causal clustering for 1-factor measurement models. In *Proceedings of the 22nd ACM SIGKDD International Conference on Knowledge Discovery and Data Mining (KDD)*, 1655–1664.
- Pearl, J. 2000. *Causality: Models, Reasoning, and Inference*. New York, NY, USA: Cambridge University Press. ISBN 0-521-77362-8.
- Pham, D. T.; and Garat, P. 1997. Blind separation of mixture of independent sources through a quasi-maximum likelihood approach. *IEEE Transactions on Signal Processing* 45(7): 1712–1725.
- Poldrack, R. A.; Laumann, T. O.; Koyejo, O.; Gregory, B.; Hover, A.; Chen, M.-Y.; Gorgolewski, K. J.; Luci, J.; Joo, S. J.; Boyd, R. L.; et al. 2015. Long-term neural and physiological phenotyping of a single human. *Nature Communications* 6(1): 1–15.
- Reilly, T.; and O’Brien, R. M. 1996. Identification of confirmatory factor analysis models of arbitrary complexity: The side-by-side rule. *Sociological Methods & Research* 24(4): 473–491.
- Shimamura, T.; Imoto, S.; Yamaguchi, R.; Nagasaki, M.; and Miyano, S. 2010. Inferring dynamic gene networks under varying conditions for transcriptomic network comparison. *Bioinformatics* 26(8): 1064–1072.
- Shimizu, S. 2012. Joint estimation of linear non-Gaussian acyclic models. *Neurocomputing* 81: 104–107.
- Shimizu, S.; Hoyer, P. O.; and Hyvärinen, A. 2009. Estimation of linear non-Gaussian acyclic models for latent factors. *Neurocomputing* 72(7-9): 2024–2027.
- Shimizu, S.; Hoyer, P. O.; Hyvärinen, A.; and Kerminen, A. 2006. A linear non-Gaussian acyclic model for causal discovery. *Journal of Machine Learning Research* 7(10): 2003–2030.
- Shimodaira, H. 2016. Cross-validation of matching correlation analysis by resampling matching weights. *Neural Networks* 75: 126–140.

- Silva, R.; Scheines, R.; Glymour, C.; and Spirtes, P. 2006. Learning the structure of linear latent variable models. *Journal of Machine Learning Research* 7(2): 191–246.
- Skitovitch, V. 1953. On a property of the normal distribution. *Doklady Akademii Nauk SSSR* 89: 217–219.
- Smith, S. M.; Miller, K. L.; Salimi-Khorshidi, G.; Webster, M.; Beckmann, C. F.; Nichols, T. E.; Ramsey, J. D.; and Woolrich, M. W. 2011. Network modelling methods for FMRI. *Neuroimage* 54(2): 875–891.
- Song, D.; Hsiao, M.-C.; Opris, I.; Hampson, R. E.; Marmarelis, V. Z.; Gerhardt, G. A.; Deadwyler, S. A.; and Berger, T. W. 2015. Hippocampal microcircuits, functional connectivity, and prostheses. In *Recent Advances On the Modular Organization of the Cortex*, 385–405. Springer.
- Spirtes, P.; Glymour, C. N.; and Scheines, R. 2000. *Causation, Prediction, and Search*. MIT press.
- Spirtes, P.; and Zhang, K. 2016. Causal discovery and inference: concepts and recent methodological advances. In *Applied Informatics*, volume 3, 3. SpringerOpen.
- Tillman, R.; and Spirtes, P. 2011. Learning equivalence classes of acyclic models with latent and selection variables from multiple datasets with overlapping variables. In *Proceedings of the 14th International Conference on Artificial Intelligence and Statistics (AISTATS)*, 3–15.
- Tillman, R. E.; and Eberhardt, F. 2014. Learning causal structure from multiple datasets with similar variable sets. *Behaviormetrika* 41(1): 41–64.
- Zheng, X.; Aragam, B.; Ravikumar, P. K.; and Xing, E. P. 2018. DAGs with NO TEARS: Continuous optimization for structure learning. In *Advances in Neural Information Processing Systems (NeurIPS)*, 9472–9483.
- Zhu, C.; Byrd, R. H.; Lu, P.; and Nocedal, J. 1997. Algorithm 778: L-BFGS-B: Fortran subroutines for large-scale bound-constrained optimization. *ACM Transactions on Mathematical Software* 23(4): 550–560.
- Zou, H.; and Hastie, T. 2005. Regularization and variable selection via the elastic net. *Journal of the Royal Statistical Society: Series B (Statistical Methodology)* 67(2): 301–320.